

Formation and Evolution of Galactic Black Holes

F. Combes

Observatoire de Paris, LERMA, 61 Av. de l'Observatoire, F-75014, Paris, France

Abstract

The main requirements for fueling an active galactic nucleus and to form massive black holes are reviewed. Low-luminosity AGN can be fueled easily from the local star clusters, near the nucleus, and the various stellar processes are described. Above a certain luminosity (and therefore accretion rate) large-scale gas flows from galactic scales are required. These can be driven by gravity torques of non-axisymmetric perturbations, such as bars, spirals, galaxy interactions. Observational evidence that these mechanisms are in action is found for high enough luminosities. It is very frequent that starbursts are also triggered through the same mechanisms, and the dense nuclear star clusters formed provide fuel for the AGN over a longer time-scale. Secular internal evolution and more violent evolution through interactions and mergers contribute to grow both a massive black hole and a bulge, and this could explain the observed proportionality relation between the mass of these two components.

Key words: active galactic nuclei, galaxies, black holes, bars, interactions

1 How to Fuel a Massive Black Hole

From the observed AGN luminosities, and an assumed conversion efficiency to transform the gravitational energy into radiation, the order of magnitudes of the accretion rates can be derived. Luminosities can be typically of the order or higher than 10^{46} erg/s. If we assume a mass-to-energy conversion efficiency $\epsilon \sim 10\%$ ($L = dM/dt c^2 \epsilon$), then the mass accretion rate dM/dt should be:

$$dM/dt \sim 1.7 (0.1/\epsilon) (L/10^{46} \text{ erg/s}) M_{\odot}/\text{yr}$$

If the duty cycle of the AGN is of the order of 10^8 yr, then a total mass up to $2 \cdot 10^8 M_{\odot}$ should be available. It is a significant fraction of the gas content of a typical galaxy, like the Milky Way! The time-scale to drive such a large mass to the center is likely to be larger than 1 Gyr.

For the mass to infall into the center, it must lose its angular momentum. Could this be due to viscous torques? In a geometrically thin accretion disk, one can consider the gas subsonic viscosity, where the viscous stress is modelled proportional (α) to the internal pressure, with a factor $\alpha < 1$. This can only gather in 1 Gyr the gas within 4α pc typically (e.g. Shlosman et al 1989, Phinney 1994). This shows that viscous torques will not couple the large-scale galaxy to the nucleus, only the very nuclear regions could play a role through viscous torques.

1.1 Stars as the AGN Fuel

The stars themselves could provide gas to the nucleus, through their mass loss, if there is a local stellar cluster, dense and compact enough (core radius R_c of less than a pc, core mass M_{core} of the order of $10^8 M_\odot$). However, the mass loss rate derived from normal stellar evolution gives only $10^{-11} M_\odot/\text{yr}/M_\odot$, orders of magnitude below the required rate of a few M_\odot/yr . The contribution will be significant, only if a massive stellar cluster ($4 \cdot 10^9 M_\odot$) has just formed through a starburst (Norman & Scoville 1988). A coeval cluster can liberate $10^9 M_\odot$ on 10^8 yr, since mainly massive stars evolve together in the beginning. Thus the existence of a starburst in the first place solves also the problem of the AGN fueling, as in the symbiotic model of Williams et al (1999). The angular momentum problem is now passed on to the starburst fueling, and could be solved only through large-scale dynamical processes.

It is also possible that stars themselves are directly swallowed by the black hole, the various processes that have been studied are:

- Bloated stars, a phenomenon that makes mass loss more efficient (Edwards 1980, Alexander & Netzer 1994, 1997),
- Tidal disruption of stars (Hills 1975, Frank & Rees 1976),
- Star Collisions (Spitzer & Saslaw 1966, Colgate 1967, Courvoisier et al 1996, Rauch 1999).

The characteristic radii associated to the prevalence of these processes are displayed in figure 1. As the black hole horizon grows faster with M_\bullet than the tidal radius, there is a limit, when $M \sim 3 \cdot 10^8 M_\odot$, above which the star disruption occurs inside the black hole, and there is no gaseous release or AGN activity (but the black hole might grow even more rapidly). This is the Hills limit (Hills 1975).

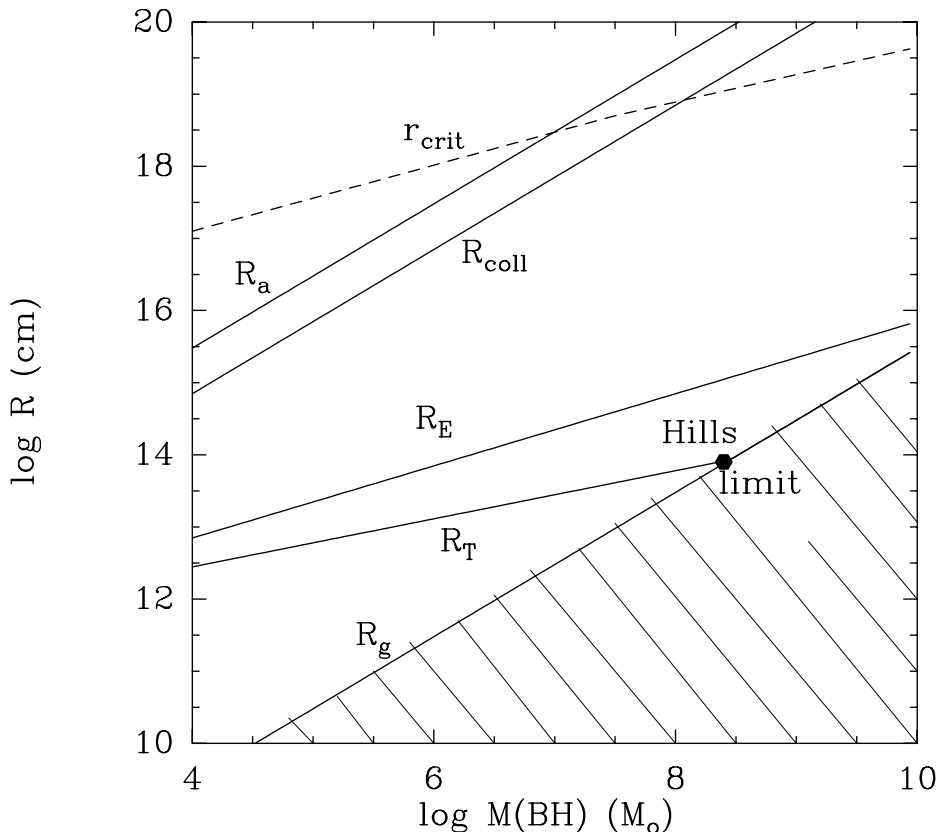


Fig. 1. Characteristic radii, corresponding to the various physical phenomena, as a function of black hole mass M_{\bullet} : from top to bottom, R_a , the accretion radius, under which the BH dominates the dynamics; R_{coll} , the collision radius, under which stellar collisions are disruptive, i.e. the free-fall velocity around the black hole $(GM_{\bullet}/r)^{1/2}$ is equal to the escape speed v_* of a typical individual star $(GM_*/r_*)^{1/2}$; R_E , the Eddington radius, under which a star receives more light than its Eddington luminosity; R_T , the tidal radius, under which a star is disrupted by the tidal forces of the BH; R_g , the gravitational radius. Loss-cone effects are important inside the critical radius r_{crit} .

1.2 Growth of Black Holes

There is now a consensus to recognize that AGN derive their power from supermassive black holes, but their formation history, their demography, their activity time-scales are still debated. The two extreme hypotheses have been explored: either only a small percentage of galaxies become quasars, and they are continuously fueled, and active over Gyrs, or a massive black hole exists in almost every galaxy, but they have active periods of only a few 10^7 yr. In the first hypothesis, there should exist black holes with masses 100 times higher than the maximum observed today, and accretion rates much lower

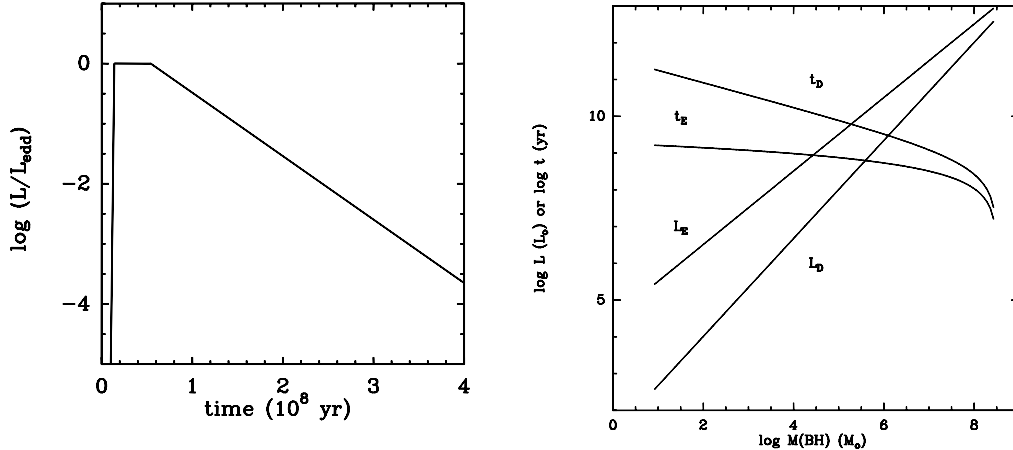


Fig. 2. **(left)** A schematic view of the activity phase of a typical quasar: during the growth phase, the AGN does not radiate efficiently, although the fueling rate is larger than Eddington. After its luminous phase of $\sim 4 \cdot 10^7$ yr, the fuel is exhausted and the AGN fades away. **(right)** Growth of a supermassive black hole in two simple models: accretion at Eddington luminosity (time-scale t_E and corresponding luminosity L_E), as a function of black hole mass M_{BH} , and when accretion is limited by diffusion (t_D and L_D) (from Hills, 1975).

than the Eddington rate, and this is not supported (e.g. Cavaliere & Padovani 1989). Models with a duty cycle of $4 \cdot 10^7$ yr are favored, and many galaxies today should host a starving black hole (Haehnelt & Rees 1993). Figure 2a schematizes the period of activity and growth of a typical massive black hole. It is also possible that further gas accretion (during a galaxy interaction for instance) triggers a new activity phase for the black hole.

If we assume that the availability of the fuel around the black hole is not a problem, then the black hole can at maximum accrete mass at the Eddington rate, and radiate at Eddington luminosity (above which the radiation pressure prevents the material to fall in). A typical growth rate for the black hole is then given by the time required to reach the critical mass M_c where $R_T = R_g$, above which stars are swallowed by the black hole without any gas radiation ($M_c = 3 \cdot 10^8 M_\odot$). The Eddington luminosity is: $L_E = 3.2 \cdot 10^4 (M/M_\odot) L_\odot$. For a mass M_c , the maximum is $10^{13} L_\odot$ (close to the peak luminosity of QSOs). Then the corresponding accretion rate, assuming an efficiency of $\epsilon = 10\text{-}20\%$ is $dM/dt_E = 1.1 \cdot 10^{-8} (M/M_\odot) M_\odot/\text{yr}$. The growth rate of the black hole in this regime t_E is then exponential; it takes only $1.6 \cdot 10^9$ yr to grow from a stellar black hole of $10 M_\odot$ to M_c :

$$t_E = 9.3 \cdot 10^7 \ln(M_c/M) \text{ yr}$$

Note that this very simple scheme would lead to a maximum at $z=2.8$ of the number of quasars. This maximum rate, however, is not realistic, since the black hole quickly gets short of fuel, as the neighbouring stars (in particular

at low angular momentum) are depleted. Then it is necessary to consider a growth limited by stellar density ρ_s :

$$DM/dt = \rho_s \sigma V$$

where σ is the accretion cross-section, and V the typical stellar velocity. The corresponding time-scale to grow from M to M_c is

$t_D = 1.7 \cdot 10^{15} \text{ yr } (\rho_s/M_\odot \text{pc}^{-3})^{-1} M/M_\odot^{-1/3} (1 - M/M_c^{1/3}) \langle V^2 \rangle^{1/2} \text{ (km/s)}$
Typically in galaxy nuclei, $\rho_s = 10^7 M_\odot/\text{pc}^3$, $\langle V^2 \rangle^{1/2} = 225 \text{ km/s}$. A black hole could grow up to M_c in a Hubble time, and the luminosity at the end could be of the order of 10^{46} erg/s (see figure 2b).

In more details, the first stars to disappear, being swallowed by the black hole, are those with the least angular momentum, with a small pericenter. The only mechanism to replenish the stellar density near the BH is the two-body relaxation, with a time-scale t_R . The relevant two-body relaxation time t_R is dependent on the number of bodies N in the system, as $t_R/t_c = N/\log N$, where t_c is the crossing time $= r_c/V$. For a galactic center, with a volumic density of stars of $10^7 M_\odot/\text{pc}^3$, this relaxation time is $3 \cdot 10^8 \text{ yr}$.

Since the angular momentum diffuse faster than the energy, the low angular momentum stars will re-appear faster, this is the loss-cone effect, that increases the accretion rate by a factor $(1 - e^2)^{-1}$, where e is the exentricity of the orbits. This is significant inside a critical radius r_{crit} , where the loss-cone angle becomes larger than the diffusion angle $\theta_D \sim (t_{dyn}/t_R)^{1/2}$. This critical radius is also plotted in figure 1.

1.3 Formation of a Cusp of Stars around the BH

From a numerical resolution of the time-dependent Boltzmann equation, with the relevant diffusion coefficients, it can be shown that around a black hole at the center of a globular cluster, the stellar density should be of a power-law shape, with a slope of 7/4, cf fig 3a (Bahcall & Wolf 1976).

The distribution of stars around a black hole can be described, according to the distance to the center:

- first for the stars not bound to the black hole, at $r > R_a$, their velocity distribution is Maxwellian, and their density profile has the isothermal power law in r^{-2} . There are also unbound stars inside R_a , but with a density in $r^{-1/2}$. This allows to compute the penetration rate of these unbound stars in the tidal or collision radius, to estimate the accretion rate. With a core stellar mass of $M_{core} = 10^7 - 3 \cdot 10^8 M_\odot$, a density 10^7 pc^{-3} , the accretion rate

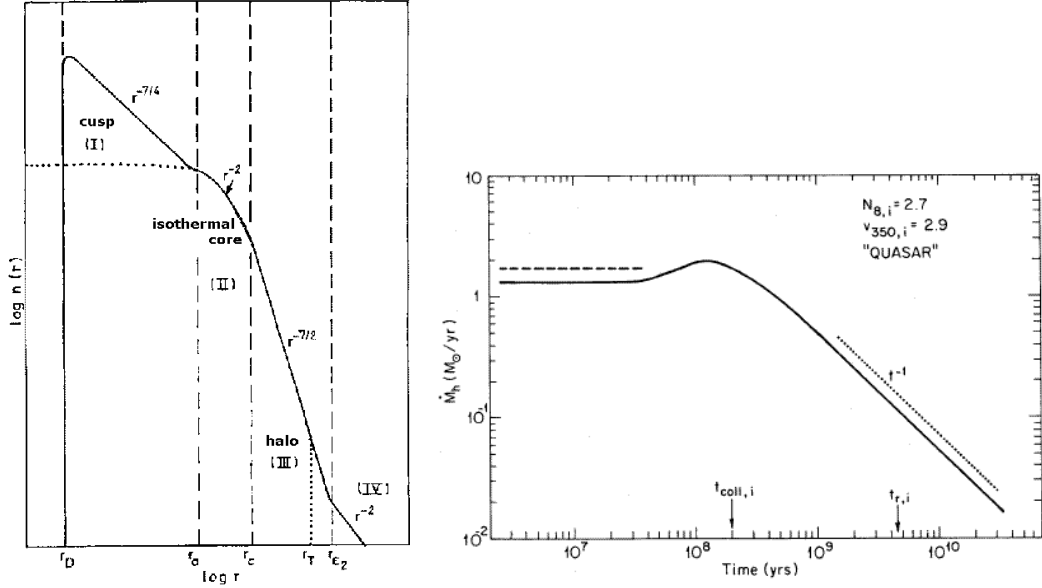


Fig. 3. **(right)** A schematic representation of the radial profile of stellar density in a spheroid with a central massive black hole. (I) the cusp, with a slope of $r^{-7/4}$, (II) an isothermal core (in r^{-2}), (III) a halo (in $r^{-7/2}$), and (IV) an isothermal tail (in r^{-2}). **(left)** the black hole growth rate, as a function of time, according to a model where the number of stars in the core is initially $2.7 \cdot 10^8$, and the velocity dispersion in the center $2.9 \times 350 = 1015$ km/s, parameters fitted to a “quasar” environment; the dash-curve is the initial rate predicted analytically (from Duncan & Shapiro, 1983).

is, by tidal disruption:

$$dM/dt_{\text{tide}} = 1 M_\odot/\text{yr} M_8^{4/3}$$

and by stellar collisions:

$$dM/dt_{\text{coll}} = 0.1 M_\odot/\text{yr} M_8^3$$

- the orbits bound to the black hole $r < R_a$: due to the cusp, their density is in $r^{-7/4}$, there is an excess of stars inside R_{coll} , that favors stellar collisions.

However, detailed numerical show that the stellar cluster cannot fuel the black hole indefinitely (Duncan & Shapiro 1983). The growth rate of the black hole and its luminosity decreases as $1/\text{time}$ (cf fig 3b). The loss-cone theory and the simulations are in agreement: the accretion rate due to tidal disruptions is M_{core}/t_R , typically of $10^{-2} M_\odot/\text{yr}$, with a maximum lower than $1 M_\odot/\text{yr}$; this cannot explain the luminosity of QSOs. QSOs might be explained only when stellar collisions are included, the corresponding accretion rate is typically a hundred times higher.

Triaxial deviations from spherical symmetry of only 5% (due to a bar or binary black hole) can repopulate the loss-cone, increasing tidal disruption to QSOs levels. However, $t_{\text{coll}} < t_R$, and collisions may destroy the cusp (Norman & Silk 1983).

Stellar collisions help to refill the loss-cone, although they flatten the stellar cusp (Rauch 1999). The collisions rate is comparable to the diffusion rate, that refill the central core.

In summary, for low density nuclei, stellar evolution and tidal disruption is the main mechanism to bring matter to the black hole, and for high density nuclei, stellar collisions dominate the gas fueling. The evolution of the stellar density through these processes is then opposite, and accentuates the differences:

- for $n < 10^7/\text{pc}^3$ the core then expands, due to heating that results from the settling of a small population of stars into orbits tightly bound to the black hole;
- for $n > 10^7/\text{pc}^3$, the core shrinks due to the removal of kinetic energy by collisions. To give an order of magnitude, the nuclear density in our own Galaxy is estimated at $10^8 M_\odot/\text{pc}^3$ (Eckart et al 1993).

These mechanisms produce differing power-law slopes in the resulting stellar density cusp surrounding the black hole, $-7/4$ and $-1/2$ for low- and high-density nuclei, respectively (Murphy et al 1991, Rauch 1999). In simulations however (Rauch 1999), collisions tend to produce a flat core, instead of $r^{-1/2}$ law in Fokker-Planck studies which imply isotropy (and are unable to treat sparse regions).

The cusps observed in nearby galaxies are consistent with the hypothesis of adiabatical black hole growth in homogeneous isothermal core (e.g. Young 1980) and with initial conditions for the cores following the scaling relations of the fundamental plane (van der Marel 1999). One must also take into account that the merging of black holes, and the dynamical effects of binary black-holes, flatten the cusp slopes (Nakano & Makino, 1999; Milosavljevic & Merritt, 2001).

1.4 Conclusion for AGN Fueling by Stars

Stars are sufficient to fuel some low luminosity AGN: there is first mass loss from a nuclear cluster, which provides only low accretion rates, then tidal disruption of stars themselves, which depletes the center, replenished through two-body relaxation. At high densities stellar collisions also replenish the central density, and the AGN can reach higher luminosities. According to the central density, the power-law slopes of the density cusp in the center are different (flatter for higher densities). However, the accretion rates reached through fueling by stars only are not sufficient to account for the most luminous AGN and quasars. Large-scale processes to transfer angular momentum of the interstellar gas over a large disk radius are then required.

2 Radial Mass Flows through Bars and Spirals

Gravity torques created in galactic disks by non-axisymmetrical perturbations, due to gravitational instabilities, can efficiently transfer the angular momentum of the interstellar gas, and help to abundantly fuel the nucleus. Numerical simulations, supported by observations, have established in the recent years that bars and spirals are density waves permanently renewed in galaxy disks.

The sign of the gravity torques, and consequent radial mass flows depend on the position of resonances, between the motions of the particles and the density wave pattern; the main features of the orbits in a barred potential and the associated resonances are now briefly recalled.

2.1 Resonances

The stellar orbits in a nearly axisymmetric potential Φ are at first order circular with an angular velocity $\Omega^2 = \frac{1}{r} \frac{d\Phi}{dr}$. In linearizing the potential in the neighborhood of a circular orbit, the motion of any particle can be expressed in first order by an epicyclic oscillation, of frequency κ ,

$$\kappa^2 = r \frac{d\Omega^2}{dr} + 4\Omega^2$$

The general orbit is therefore the combination of a circle and an epicycle, or a rosette, since there is no rational relation between the two periods.

The bar creates a bisymmetric gravitational potential, with a predominant Fourier component $m = 2$, which rotates in the galaxy with the pattern speed Ω_b . There is a region in the plane where the pattern speed is equal to the frequency of rotation Ω , and where particles do not make any revolution in the rotating frame. This is the resonance of corotation (cf fig 4).

Periodic orbits in the bar rotating frame are orbits that close on themselves after one or more turns. Periodic orbits are the building blocks which determine the stellar distribution function, since they define families of trapped orbits around them. Trapped orbits are non-periodic, but oscillate about one periodic orbit, with a similar shape. The various families are (Contopoulos & Grosbøl 1989):

- the x_1 family of periodic orbits is the main family supporting the bar. Orbits are elongated parallel to the bar, within corotation. They can look like simple ellipses, and with energy increasing, they can form a cusp, and even two loops at the extremities.

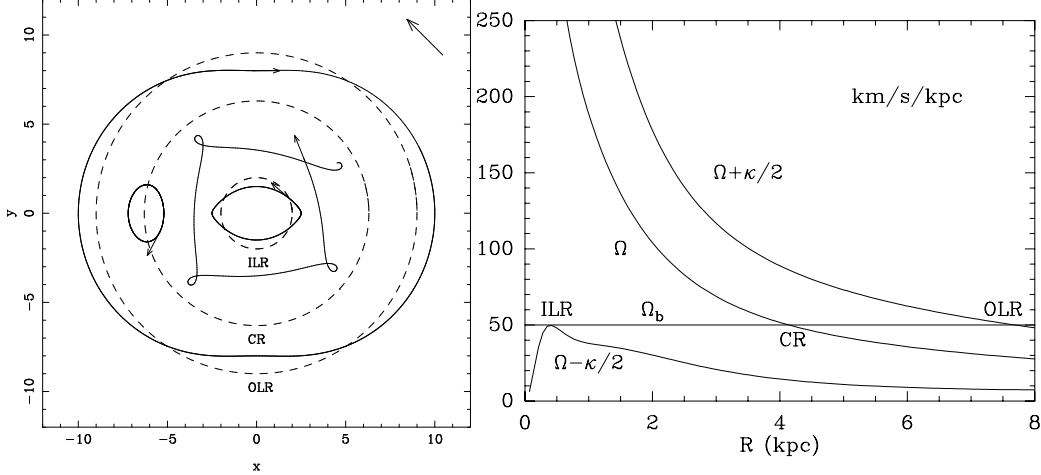


Fig. 4. **left**: Various types of resonant orbits in a galaxy. At the ILR, the orbit is closed and elongated, and is direct in the rotating frame. At Corotation (CR), the orbit makes no turn, only an epicycle; at OLR, the orbit is closed, elongated and retrograde in the rotating frame. In between, the orbits are rosettes that do not close. **right**: Frequencies Ω , $\Omega - \kappa/2$ and $\Omega + \kappa/2$ in a galaxy disk. The bar pattern speed Ω_b is indicated, defining the locations of the Lindblad resonances.

- the x_2 family exists only between the two inner Lindblad resonances (ILR), when they exist. They are more round, and elongated perpendicular to the bar. Even when there exist two ILRs in the axisymmetric sense, the existence of the x_2 family is not certain. When the bar is strong enough, the x_2 orbits disappear. The bar strength necessary to eliminate the x_2 family depends on the pattern speed Ω_b : the lower this speed, the stronger the bar must be.
- Outside corotation, the 2/1 orbits (which close after one turn and two epicycles) are run in the retrograde sense in the rotating frame; they are perpendicular to the bar inside the outer Lindblad resonance (OLR), and parallel to the bar slightly outside.

In summary, the orientation of the periodic orbits rotates by 90° at each resonance crossing, and they are successively parallel and perpendicular to the bar. The gas will first tend to follow these orbits, but the streamlines of gas cannot cross. Since periodic orbits do cross, gas clouds can encounter enhanced collisions, such that their orbits are changed. Instead of experiencing sudden 90° turns, their orbits will smoothly and gradually turn, following the schematic diagram of kinematic waves, first drawn by Kalnajs (1973), and illustrated in fig 5.

This interpretation predicts that the arms will be more wound when there exist more resonances; there will be a winding over 180° with only CR and OLR, with the gas aligned with the bar until corotation. When there exists 2 ILRs, the gas response can be perpendicular to the stellar bar.

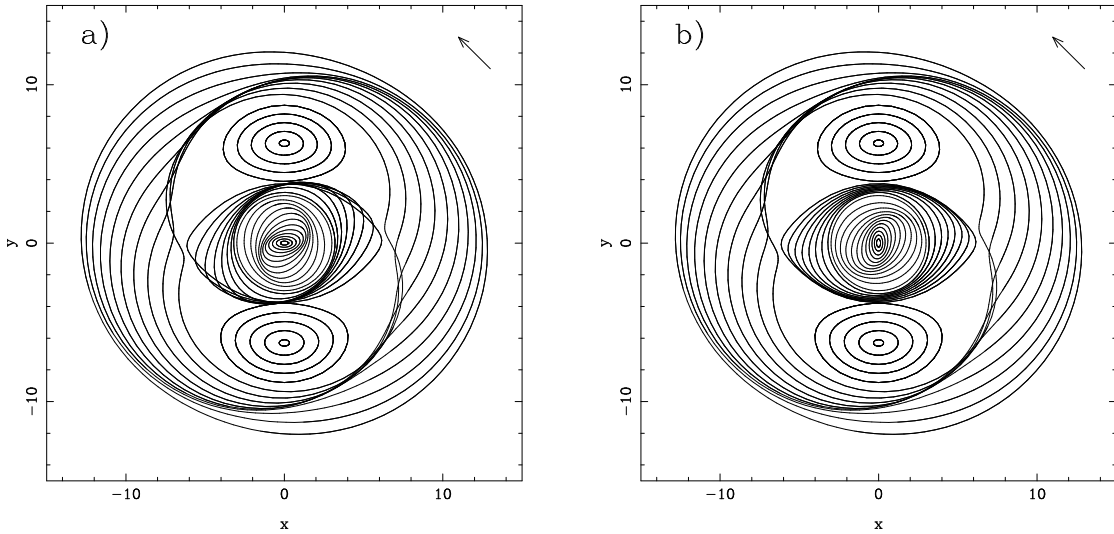


Fig. 5. Behaviour of the gas flow in a barred galaxy ($\cos 2\theta$ potential, oriented horizontally). The gas tends to follow the periodic orbits whose orientation rotates by $\pi/2$ at each resonance. Due to dissipation, the gas orientation change gradually. The sense of winding can be derived from the variation of the precession rate $\Omega - \kappa/2$ as a function of radius: **a)** Without a central mass concentration, $\Omega - \kappa/2$ is increasing with radius in the center: the gas winds up in a leading spiral inside the ILR ring; **b)** with a central mass concentration, it is the reverse and the gas follows a trailing spiral structure, inside ILR.

2.2 Angular Momentum Transfer

To minimize its total energy, a galaxy tends to concentrate its mass towards the center, and to transfer its angular momentum outwards (Lynden-Bell & Kalnajs 1972). It is the role of the spiral structure to transport angular momentum from the center to the outer parts, and only trailing waves can do it. This transfer, mediated by non-axisymmetric instabilities, is the motor of secular evolution of galaxies, and of the formation of bars and resonant rings.

The angular momentum transfer is due to the torques exerted by the bar on the matter forming spiral arms. There is a phase shift between the density and the potential wells, resulting in torques schematized in fig 6. The gas is much more responsive to these torques, since they form the spirals in a barred galaxy. The torque changes sign at each resonance, where the spiral turns by 90° . Between the ILR and corotation, the torque is negative, while between CR and OLR, the torque is positive. These torques tend to depopulate the corotation region, and to accumulate gas towards the Lindblad resonances, in the shape of rings. Indeed, these rings then are aligned with the symmetry axis of the bar, and no net torque is acting on them. Numerical simulations of colliding gas clouds in a barred potential show that rings form in a few dynamical times, i.e. in a few Gyrs for the outer ring at OLR (Schwarz 1981),

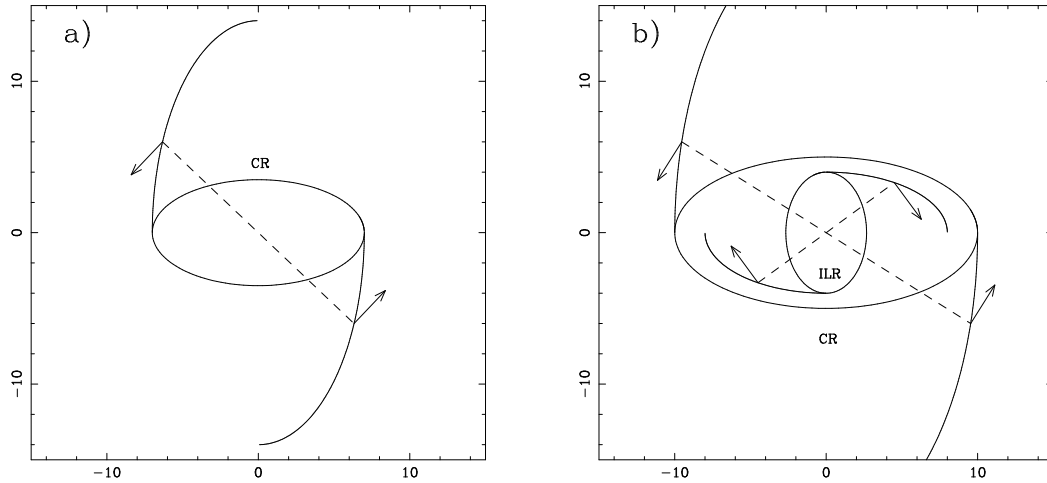


Fig. 6. Schematic representation of the gravity torques exerted by the bar on the gaseous spiral: **a)** between CR and OLR, the gas acquires angular momentum and is driven outwards; **b)** between CR and ILR, the gas loses angular momentum (cf Combes 1988).

or in $\sim 10^8$ yr for nuclear rings at ILR (Combes & Gerin 1985).

2.3 Fueling Nuclear Activity

The main issue to fuel the nucleus is to solve the transfer of angular momentum problem. Torques due to the bar are very efficient, but gas can be stalled in a nuclear ring at ILR. Other mechanisms can then be invoked: viscous torques, or dynamical friction of giant clouds (GMC) against stars. The viscosity is in general completely unefficient over the galactic disk, but the corresponding time-scale is decreasing with decreasing radius. Unfortunately, in the center of galaxies, the rotation is almost rigid, the shear is considerably reduced, and so are the viscous torques. The time-scale for dynamical friction becomes competitive below $r=100\text{pc}$ from the center (about $10^7 (r/100\text{pc})^2$ yr for a GMC of $10^7 M_\odot$). For the intermediate scales, a new mechanism is required.

Note that if there is a supermassive black hole in the nucleus, it is easier to bring the gas to the center. Indeed, the presence of a large mass can change the behaviour of the precessing rate of orbits $\Omega - \kappa/2$: instead of increasing with radius inside ILR (as in fig 4), it will decrease.

Due to cloud collisions, the gas clouds lose energy, and their galactocentric distance shrinks. Since it tends to follow the periodic orbits, the gas streams in elliptical trajectories at lower and lower radii, with their major axes leading more and more the periodic orbit, since the precession rate (estimated by

$\Omega - \kappa/2$ in the axisymmetric limit, for orbits near ILR, and by $\Omega + \kappa/2$ near OLR) increases with decreasing radii in most of the disk (fig 5). This regular shift forces the gas into a trailing spiral structure, from which the sense of the gravity torques can be easily derived. Inside corotation, the torques are negative, and the gas is driven inwards towards the inner Lindblad resonance (ILR). Inside ILR, and from the center, the precession rate is increasing with radius, so that the gas pattern due to collisions will be a leading spiral, instead of a trailing one (see Figure 5a). The gravity torques are positive, which also contributes to the accumulation of gas at the ILR ring. This situation is only inverted in the case of a central mass concentration (for instance a black hole), for which the precession rate $\Omega - \kappa/2$ is monotonically increasing towards infinity with decreasing radii. Only then, the gravity torques will pull the gas towards the very center, and “fuel” the nucleus.

The problem reduces to forming the black hole in the first place. We show next that the accumulation of matter towards the center can produce a decoupling of a second bar inside the primary bar. This nuclear bar, and possibly other ones nested inside like russian dolls, can take over the action of gravity torques to drive the gas to the nucleus, as first proposed by Shlosman et al. (1989).

2.4 Decoupling of a Nuclear Disk and/or Bar

The bar torques drive progressively more mass towards the center. This matter, gaseous at the beginning, forms stars, and gradually contributes to the formation of the bulge, since stars are elevated above the disk plane, through vertical resonances with the bar (e.g. Combes et al. 1990, Raha et al. 1991). When the mass accumulation is large enough, then the precession rate $\Omega - \kappa/2$ curve is increasing strongly while the radius decreases, and this implies the formation of two inner Lindblad resonances. In between the two ILRs, the periodic orbits are perpendicular to the bar (x_2 orbits), and the bar loses its main supporters. The weakening of the primary bar, and the fact that the frequencies of the matter are considerably different now between the inner and outer disk, forces the decoupling of a nuclear disk, or nuclear bar from the large-scale bar (primary bar).

Nuclear disks are frequently observed, at many wavelengths: optical or NIR with the HST (e.g. Barth et al 1995, Regan & Mulchaey 1999), see also fig 7), or in CO molecules with millimeter interferometers (Ishizuki et al 1990, Sakamoto et al 1999). A recent survey in the Virgo cluster (Rubin et al 1997) reveals that about 20% of the 80 spirals observed possess a decoupled nuclear disk. The stellar nuclear disk is kinematically cold, which suggest a recent formation from gas (Emsellem et al. 2001). The percentage of double-barred galaxies is observed around 20% (Wozniak et al. 1995, Jungwiert et al 1997,

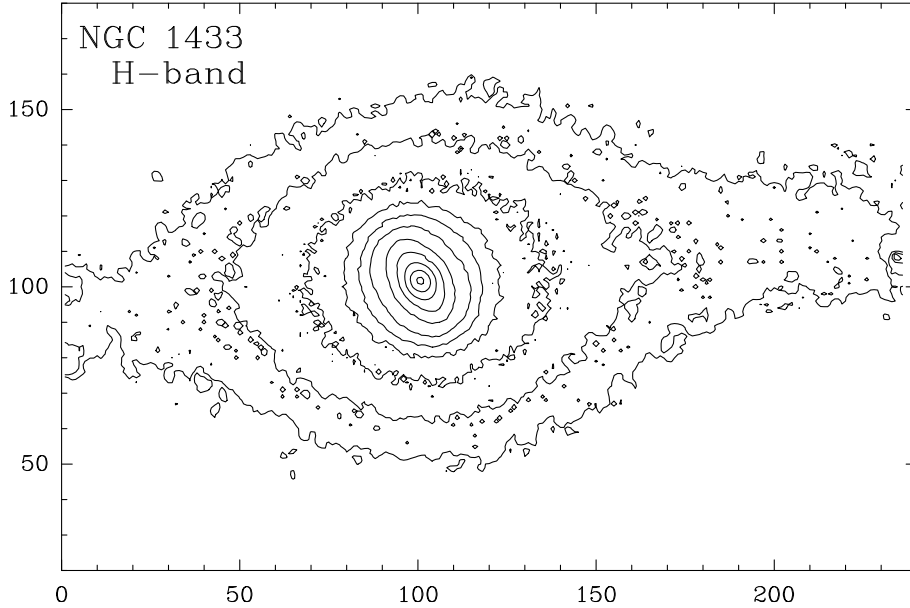


Fig. 7. Example of a nuclear bar seen in the NIR H band: the Seyfert 2 barred spiral galaxy NGC 1433. The pixel size is $0.52''$, from Jungwiert et al. (1997)

Laine et al 2002).

2.5 Bar Destruction and Renewal

The inflow of matter in the center can destroy the bar. It is sufficient that 5% of the mass of the disk has sunk inside the inner Lindblad resonance (Hasan & Norman 1990, Pfenniger & Norman 1990, Hasan et al 1993). But this depends on the mass distribution, on the size of the central concentration; a point mass like a black hole is more efficient (maybe 2% is sufficient). The destruction is due to the mass re-organisation, that perturbs all the orbital structure: the x_1 orbits sustaining the bar for instance are shifted outwards. Near the center, the central mass axisymmetrizes the potential. Then there is a chaotic region, and outside a regular one again. When a central mass concentration exists initially, in N-body simulations, a bar still forms, but dissolves more quickly. It is also possible that after a bar has dissolved, another one forms, after sufficient gas accretion to generate new gravitational instabilities: the location of the resonances will not be the same (Bournaud & Combes 2002).

There might be several bar episodes in a galaxy disk, with secondary bars transiently prolonging the action of the primary bars. The succession of bars follow a self-regulated process, based on gravitational instability, and disc cooling through the gas dissipation. When a strong bar is developing, the gas inside corotation is driven inwards, and produce a central concentration that progressively tends to weaken or destroy the bar. At the same time, gas

from the outer parts is held outside, since gravity torques are positive there. When the bar disappears, gas can then infall from the outer parts, and settles in the disk, that becomes unstable again to bar formation, etc..

When gas is driven inwards, it can fuel a starburst there, and then the central black hole. The vertical resonances help also to grow the bulge, in parallel to the black hole (e.g. Combes 2000).

3 Are there Correlations between Bars and AGN?

There have been several observational works revealing a correlation between nuclear activity and bars (Dahari 1984, Simkin et al 1980) or between activity and distorted morphologies (Moles et al 1995). But the correlation is weak and depends on the definition of the samples, their completion and other subtle effects. Near-infrared images have often revealed bars in galaxies previously classified unbarred, certainly due to gas and dust effects. However, Seyfert galaxies observed in NIR do not statistically have more bars nor more interactions than a control sample, cf fig 8 (McLeod & Rieke 1995, Mulchaey & Regan 1997).

It is however evident from observations that bars are efficient to produce radial gas flows: barred galaxies have more H_2 gas concentration inside their central 500 pc than un-barred galaxies (cf Sakamoto et al 1999). Also, the radial flows level out abundance gradients in barred galaxies (Martin & Roy 1994).

Peletier et al (1999) and Knapen et al (2000) have recently re-visited the question, and find that Seyfert galaxies are more barred than non-Seyfert, a result significant at at 2.5σ . They measure the bar strength by the observed axial ratio in the images. In Seyferts, the fraction of strong bars is lower than in the control sample (Shlosman et al. 2000). Although a surprising result a priori, this is not unexpected, if bars are believed to be destroyed by central mass concentrations (cf section 2.5). Regan & Mulchaey (1999) have studied 12 Seyfert galaxies with HST-NICMOS. Out of the 12, only 3 have nuclear bars but a majority show nuclear spirals. However their criterium for nuclear bars is that there exist leading dust lanes along this nuclear bar. This is not a required characteristic, since these secondary bars in general are not expected to have ILRs themselves. Circumnuclear dust and nuclear spirals are frequently found, a striking result from HST color images (Martini & Pogge 1999, Pogge & Martini 2002).

The frequency of nuclear bars happen to be the same (of the order of 20-30% in active and non-active galaxies (Regan & Mulchaey 1999, Laine et al 2002).

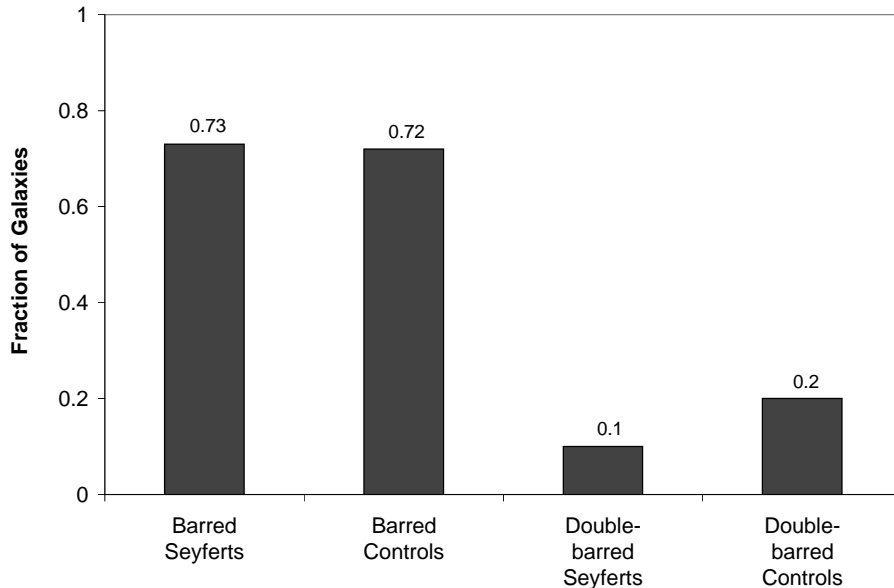


Fig. 8. Fraction of barred and double-barred systems in the Seyfert and control galaxy samples. The percentage of barred galaxies is comparable in the Seyfert and control samples. A slightly higher percentage of the normal galaxies have double bars (from Mulchaey & Regan 1997).

If there is no correlation, this could be due to the fact that a strong bar is not sufficient to trigger nuclear activity, there should exist also a massive black hole in the center, and this favors the early-type galaxies. Indeed, there is a correlation between the mass of the bulge and that of the BH, and also, the fueling mechanism requires a central mass concentration to be efficient (see previous section). Observationally, there is a good correlation between AGN and morphological types: AGN tend to lie in early-type galaxies (Terlevich et al 1987, Moles et al 1995, Ho et al 1997). The lack of correlation could also be related to the variable gas content near the center. However, there does not appear to be more circumnuclear dust in Seyfert galaxies with respect to non active galaxies (Pogge & Martini 2002).

A morphological study of the 891 galaxies in the Extended 12 μm Galaxy Sample (E12GS) has confirmed that Seyfert galaxies and Liners have the same percentage of bars as normal spirals, contrary to HII/Starburst galaxies that have more bars (Hunt & Malkan 1999). However, active galaxies show rings significantly more often than normal galaxies or starbursts. The Liners have more inner rings (by a factor 1.5), while Seyferts have more outer rings (by a factor 3-4) than normal galaxies. This might be due to the different time-

scales for bar and ring formation: bars form relatively quickly, in a few 10^8 yr; they can drive matter to the central regions and trigger a starburst there, in the same time-scale. Outer rings form then, also under the gravity torques of the bar, but in the dynamical times of the outer regions, i.e. a few 10^9 yr. Since Seyferts are correlated with them, they would be associated to delayed consequences of the starburst, or of the bar, which by this time begins to dissolve.

The percentage of AGN in the E12GS sample is 30%. As for interactions, 25% of the Seyferts are "peculiar" (disturbed), while 45% of the HII/Starbursts are. There is also a correlation between AGN and morphological types along the Hubble sequence. Seyferts tend to lie in early-types (Terlevich et al 1987, Moles et al 1995). This has to be related to the existence on inner Linblad resonances in early-types, favoring the fueling of the nucleus (e.g. section 2.3, Combes & Elmegreen 1993). In summary, there might be some evidence of the role of large-scale dynamics on AGN fueling, but it is in general weak, except for the most powerful AGN. A good correlation between bars/interactions and AGN is not expected, from several arguments:

- there must be already a massive black hole in the nucleus, and this might be the case only for massive-bulge galaxies (not all barred galaxies)
- again a large central mass concentration (bulge) is necessary to produce an ILR and drive the gas inwards (early-types)
- other parameters, like geometrical parameters, control the fueling efficiency of interaction
- time-scales are not fitted: the AGN fueling is postponed after the interaction/bar episode
- there are other mechanisms to fuel AGN such that a dense nuclear cluster

4 Galaxy Interactions and Merging

Galaxy interactions create also strong non-axisymmetries in galaxy disks, and are an efficient way to transfer angular momentum. They trigger strong bars in the interacting galaxy disks (e.g. Barnes & Hernquist 1992) and drive the gas inwards through the same mechanisms as described before (section 2.2). Again, the fueling is dependent on the morphological type of the galaxy, since the stability of disks is essentially dependent on the bulge-to-disc ratio (Mihos & Hernquist 1994, 1996). Numerical simulations have shown that the star formation rate is considerably enhanced in galaxy interactions, because of the gas

concentration (the star formation is locally proportional to the gas density), and to the orbit crowding (shocks favoring the dissipation of gas). When the time-scale of radial gas inflow is smaller than the star-formation feedback (through supernovae, stellar winds, etc.), huge starbursts may occur.

There is indeed a very good correlation between high luminosity starbursts and galaxy interactions and mergers (e.g. Sanders & Mirabel 1996). For the most luminous objects, a significant fraction of their luminosity is coming from nuclear activity, and this fraction is increasing with infrared luminosity, from 4 to 45% (Kim et al 1998). QSOs appear more than usual to interact with companions (Hutchings & Neff 1992; Hutchings & Morris 1995). For AGN of low luminosity, external triggering appears less necessary, since only $0.01 M_{\odot}/\text{yr}$ is required for a Seyfert like NGC 1068 for example, during 10^8 yr. However, once interactions drive gas to the nucleus, some activity must be revived. Time-scales may be the reason why the actions are not simultaneous. Large-scale gas has to be driven at very small scales in the center, and the whole process requires several intermediate steps.

Even for the good starburst/interactions correlations, there are exceptions for the low- luminosity samples. Interacting galaxies selected optically (not IRAS galaxies) are often not enhanced in star formation (Bushouse 1986, Lawrence et al 1989). Only the obviously merging galaxies, like the Toomre (1977) sample, are truly a starbursting class; it is difficult to reveal a progression along a possible evolutionary sequence (Heckman 1990). There are too many determining parameters: geometry, distance, gas content, etc...

A complication comes from the time-scales involved: the starburst phase is short, of the order of a few 10^8 yr, similar only to the end of the merging phase. It is more the presence of morphological distortions than the presence of nearby companions that is correlated with activity. More than 50% of ULIRGS possess multiple nuclei (Carico et al 1990, Graham et al 1990).

Are Seyfert galaxies preferentially interacting? According to Dahari (1984), 15% have close companions, compared to 3% in the control sample. But the Seyferts with or without companions have the same $H\alpha$ or radio power (Dahari 1985), although they may be more infrared bright with companions (Dahari & DeRobertis 1988, McKenty 1989). According to Keel et al (1985), there are 5% of Seyferts in control sample, and 25% in the close pairs of Arp Atlas. But it is possible that the Arp Atlas galaxies suffer from selection effects. Bushouse (1986) and deRobertis et al 1996) on the contrary finds a deficiency of Seyferts in interacting galaxies. A recent study by Schmitt (2001) finds no statistical difference in companion frequency for the various activity types: Seyfert, Liners, transition, III. The claim that Seyfert 2 have a larger number of companions than Seyfert 1 (Laurikainen & Salo 1995, Dultzin-Hacyan et al 1999) was not confirmed by all studies (Schmitt et al 2001); this could be an

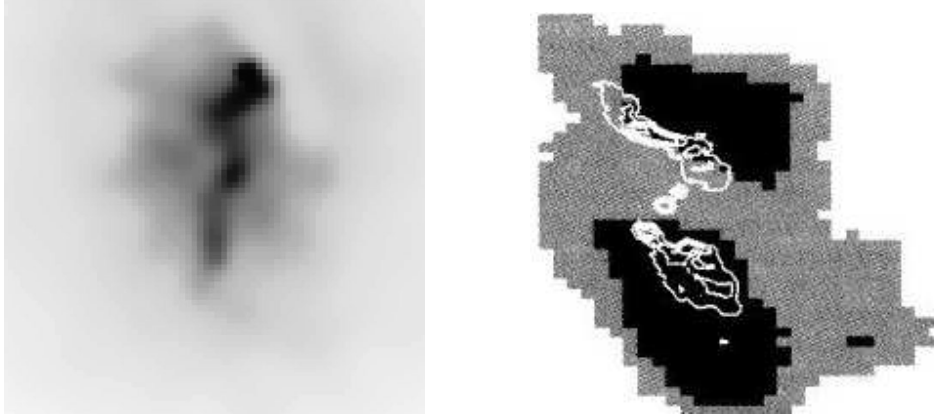


Fig. 9. **left** X-ray Chandra picture of the cooling flow at the center of the galaxy cluster Abell 1795 (Fabian et al. 2001). The filament is about 40kpc in length. **right** The cooling flow interacts at its base with the radio lobes, here represented in contours, of the central radio source; the grey-scale indicates the presence of blue-color regions, here in two patches at about 6 kpc from the nucleus, just beyond the radio lobes (from Fabian 1994).

artifact, some Seyfert 2 have an UV excess due to a starburst (Cid Fernandes et al 1998), and companions enhance the star formation rate.

Another fueling mechanism could be the cooling flows that are expected to be infalling in the center of rich clusters. Indeed, it is frequent that AGN are present in the cluster central galaxies. They are frequently powerful radio-sources, and the radio-lobes might be a heating/regulating process of the cooling gas (Fabian et al. 2001). The example of Abell 1795 in figure 9 is illustrative of the phenomenon.

In summary, if the environment influence is evident for powerful QSOs, Radio-galaxies and BILacs, it is not so significant for Seyferts.

5 Galaxy Encounters and Binary BH Formation

Given the large frequency of galaxy encounters and mergers, if there is a massive black hole in nearly every galaxy, the formation of a binary black hole should be a common phenomenon. The successive physical processes able to brake the two black holes in their relative orbit have been considered by Begelman et al (1980).

5.1 Physical Processes Involved

Each black hole sinks first toward the merger remnant center through dynamical friction onto stars. A binary is formed; but the life-time of such a binary can be much larger than a Hubble time, if there is not enough stars to replenish the loss cone, where stars are able to interact with the binary. Once a loss cone is created, it is replenished only through the 2-body relaxation between stars, and this can be very long (see section 1). Modelling the merger remnant as an elliptical, with a core of radius r_c and mass M_c (and corresponding velocity V_c), the radius where loss cone effects are significant is: $r_{lc}/r_c = (M_{bh}/M_c)^{3/4}$. The various time-scales involved, and corresponding characteristic scales are defined by the following steps:

- the dynamical friction on stars, in less than a galactic dynamical time,

$$t_{df} \sim (V_c/300\text{km/s})(r_c/100\text{pc})^2(10^8/M_{bh}) \text{ Myr}$$

- when the separation of the binary shrinks to a value $r_b = r_c(M_{bh}/M_c)^{1/3}$, the two black holes become bound together
- the binary hardens, with $r_h \propto (r/r_b)^{3/2}$
- but when $r < r_{lc} = (M_{bh}/M_c)^{3/4}r_c$, the stars available for the binary to interact with, are depleted through the loss cone effect, and replenished only by 2-body relaxation
- gas infall can reduce the binary life-time (whether the gas is flung out, or accreted, there is a contraction of the binary) in t_{gas}
- gravitational radiation shrinks the orbit on $t_{GR} \sim 0.3\text{Myr}(10^8/M_{bh})^3(r/0.003\text{pc})^4$ if the two black holes have comparable masses

5.2 Life-time of the Binary

If the binary life-time is too long, another merger with another galaxy will bring a third black-hole. Since a three-body system is unstable, one of the three black-holes will be ejected by the gravitational slingshot effect.

Since the life-time of the binary is not short, there should be observable manifestations of massive black hole binaries. One of the best tracer is to detect the periodicity of the keplerian motion, with the period $P \sim 1.6\text{yr} r_{16}^{3/2} M_8^{-1/2}$. This is the case for the AGN OJ 287 where eclipses have been monitored for a century (Takalo 1994, Lehto & Valtonen 1996, Pietilä 1998). Also, if the black holes are rotating, and their spins have misaligned axes, they precess around the orbital one. Plasma beams (aligned to the hole axis) precess, and curved jets should be observed, with periods between 10^3 to 10^7 yr. This is frequently the case in radio structures observed with VLA and VLBI, modified

by Doppler boosting, and light travel time (cf 3C 273, NGC 6251, 1928+738, Kaastra & Roos 1992; Roos et al 1993). Finally, pairs of radio galaxies have been observed during their merger with four radio jets (3C75, Owen et al 1985).

Numerical simulations have brought more precision in the determination of the life-time of the binary, although numerical artifacts have given rise to debates. Ebisuzaki et al (1991) claimed that the life-time of the binary should be much shorter if its orbit is excentric, since then the binary can interact with more stars and release the loss cone problem. The first numerical simulations tended to show that orbit excentricity should grow quickly through dynamical friction (Fukushige et al 1992). Mikkola & Valtonen (1992) and others found that the excentricity in fact grows only very slowly.

To summarize the conclusions of several numerical computations, there is finally little dependence on excentricity e , only in rare cases, when e is large from the beginning (Quinlan 1996). Eventually, the wandering of the binary helps the merging of the two black holes (Quinlan & Hernquist 1997). The ejection out of the core of stars interacting with the binary weakens the stellar cusp, while the binary hardens. This may help to explain the surprisingly weak stellar cusps in the center of giant ellipticals observed recently with HST. Observations show that bright elliptical galaxies have weak cusps, while faint galaxies have strong cusps, with a power law slope of density versus radius of up to 2. A way to weaken the cusps is a sinking black hole (Nakano & Makino 1999), or binary black holes (Milosavljevic & Merritt, 2001) and this could be the case for giant galaxies that have experienced many mergers in their life.

5.3 Conclusions on BH Binaries

Binary black holes form efficiently during galaxy mergers, due to dynamical friction, in time-scales of 10-100 Myr. The life-time of the binary is quite variable, and can be significantly shortened by gas accretion. The slingshot effect could reduce the number of massive black holes, but appears unlikely.

The rate of black holes merging is important to estimate the possible detection rate of gravitational waves: if only bright AGN are taken into account, this rate is below 0.1 per year. however, with a massive black hole in every galaxy with spheroid, this rate reaches a few per year. Massive black holes explain the formation of cusps in the stellar density in the center of galaxies, while binary black holes are needed to flatten the cusp slopes.

6 Cosmic Density of BH and Evolution with Redshift

6.1 Comparison with the Background Radiations

An important observational result, from kinematical studies with high spatial resolution in nearby galaxies has been the existence of a black hole in each bulge/spheroid galaxy, with a proportionality factor between the mass of the BH and that of the bulge: $M_{BH} = 0.002 M_b$ (Magorrian et al 98) or an even better correlation with the central stellar velocity dispersion (Ferrarese & Merritt 2000, Gebhardt et al. 2000). From this it is possible to deduce the density of black hole in the universe (given the baryonic density of the Universe). If we assume that this amount of mass of black hole has radiated while growing (i.e. masses of black holes are not above the Hills's limit), then it is interesting to compare the derived radiation density expected in the Universe from the formation of black holes. This comparison with the cosmic background radiations (e.g. Haehnelt et al. 1998), assuming black holes radiate at Eddington luminosities, reveals that essentially the cosmic infra-red radiation is compatible with what expected from the present black hole density, assuming that a fraction of 30% of it comes from AGN and the rest from starbursts. The optical cosmic background radiation is observed much lower, and suffers certainly from high obscuration.

6.2 Evolution of the BH Mass in Active Galaxies

Another observational data, to be taken into account to reproduce the formation of massive black holes, is the redshift evolution of the density of quasars, and the derived black hole masses. It is well known that the optically-selected quasars, but also the radio-loud quasars were more abundant in the past (Shaver et al 1996), and their evolution curve follows that of the density of starburst, or the star formation history (cf fig 10b). Given the luminosity function of AGN (Boyle et al 1991), and assuming they are radiating at Eddington luminosity, a distribution of black hole mass can be derived. This shows that active galaxies in the past had in average larger black hole masses (Haehnelt & Rees 1993).

Of course, the mass of a given black hole only increases with time, but those which went through their active AGN phase in the past were of larger mass, because of a more abundant fueling, possibly due to the gas richness, and the shortest dynamical time in denser galactic systems. At the present time, only low-mass spheroids (with low-mass BH) have sufficient gas in their environment to become active. The large-mass black holes, in big early-types objects

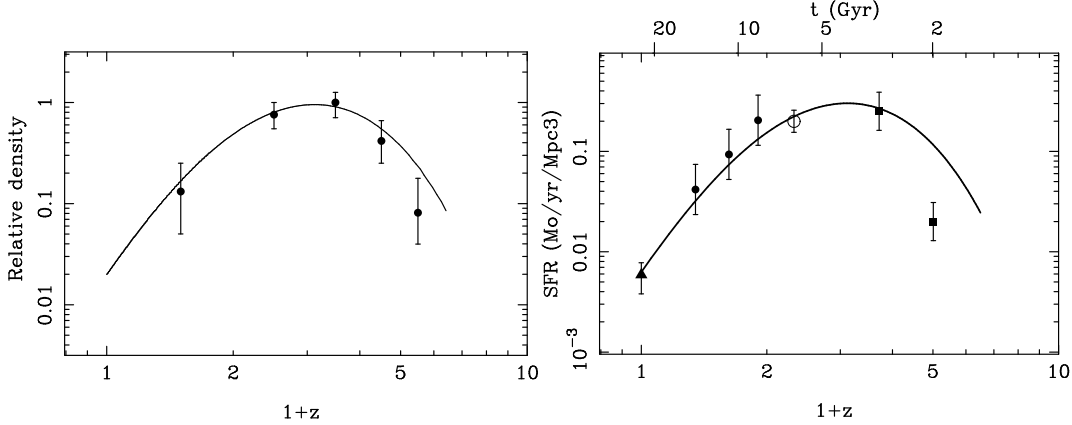


Fig. 10. **left** Space density as a function of redshift, normalised to $z = 2 - 3$, for the Parkes flat-spectrum radio-loud quasars with $P_{11} > 7.2 \cdot 10^{26} \text{ W Hz}^{-1} \text{ sr}^{-1}$. The optically-selected quasars follow the same curve (from Shaver et al. 1996). **right** Cosmic history of star formation, for comparison. The various data points, coming from different surveys, give the universal metal ejection rate, or the star formation rate SFR (left-scale), as a function of redshift z .

like massive ellipticals, are starving.

7 Modelisation

Semi-analytic models, based on the Press-Schechter formalism, and a CDM hierarchical scenario of galaxy formation (Kauffmann & Haehnelt 2000), can reproduce rather well the essential observations: the proportionality relation between the bulge and black hole mass in every galaxy, the amount of energy radiated over the Hubble time due to accretion onto massive black holes, the past evolution of AGN activity. The assumptions are that the black holes grow through galaxy merging, both because of the merger of the pre-existing black holes, and due to the infall of gas to the center in the merging, that can fuel the merged BH. It is also assumed that the cold gas in galaxies decrease with time; this implies that the fueling will also decrease with time, accounting for the observed decline of AGN activity. Finally, the gas accretion time-scale is proportional to the dynamical time-scale, which is shorter at high redshift. The quasars convert mass to energy at a fixed efficiency, and cannot radiate more than the Eddington limit.

The results of such simulations are a strong decrease of the gas fraction in galaxies, from 75% at $z=3$ to 10% at $z=0$, corresponding to the gas density decrease observed in the damped Lyman alpha systems (e.g. Storrie-Lombardi & Wolfe 2000); this implies that the black holes in the smallest ellipticals that formed at high z are relatively more massive, since there was more gas at this epoch. Ellipticals forming today have smaller black holes. Also the brightness

of AGN for a given galaxy was relatively higher in the past. The rapid decline of quasars is then due to several causes:

- a decrease in the merging rate (which is also the cause of the decrease of the star formation rate)
- the decrease of the gas mass fraction in galaxies, due to the consumption by stars
- the increase of the accretion time-scales (the dynamical processes are slower, for a given amount of fuel)

In these kind of models, it is natural to expect a ratio of proportionality between bulge and black hole masses, since they both form from the same mechanisms, the hierarchical merging, and the corresponding dynamical gas concentration. It is interesting to note that the life-time of the quasar phase, a few 10^7 yr is then derived.

8 Conclusions

The rapid decline of AGN from $z=2$ to $z=0$ is parallel to that of the star formation history, and is likely to have the same causes. Since black hole masses have accumulated in the center of each galaxy at the present time, the main reason for the lower activity is the shortage of fuel. AGN are accreting today at a rate much lower than Eddington rate. The dominant active nuclei are presently low-luminosity AGN (Seyferts), revived by gas accretion from galaxy interactions, much less frequent than in the past. Also the galaxies with higher gas fraction are late-type galaxies, that have small-mass black holes in their nuclei.

Spheroids and massive black holes appear to be formed with the same mechanisms. Mass concentration is enhanced by radial gas flows, driven from the galactic disks, through density waves, such as bars and spirals. Internal gravity torques and non-axisymmetries are also boosted by galaxy interactions and mergers. Gas fueling towards the center can trigger nuclear starbursts, forming dense compact nuclear stellar clusters, that in turn will fuel a massive black hole. The detailed processes regulating the successive/alternate fueling of starbursts and BH are not yet completely elucidated, and might involve the stability of galactic disks, the depth of the central potential well.

The required fueling depends on the strength and luminosity of the AGN. For Seyferts, only stars from a dense nuclear cluster are sufficient, through tidal disruptions and stellar collisions. For quasars, big starbursts are required, and the coeval compact cluster just formed can provide the fuel through mass loss of young stars and supernovae.

The relations between BH and bulge masses, or with the central velocity dispersion, are then naturally explained by the complicity between starbursts and AGN.

References

- Alexander T., Netzer N.: 1994, MNRAS 270, 781
Alexander T., Netzer N.: 1997, MNRAS 284, 967
Bahcall, J. N., Wolf, R. A.: 1976, ApJ 209, 214
Barnes J.E., Hernquist L.: 1992, ARAA 30, 705
Barth A., Ho L. C., Filippenko, A. V., Sargent, W. L.: 1995, AJ 110, 1009
Begelman M.C., Blandford R.D., Rees M.J.: 1980, Nature 287, 307
Bournaud, F., Combes, F. 2002, A&A, in press (astro-ph/0206273).
Boyle B.J., Jones L.R., Shanks T. et al.: 1991, in “The Space Density of Quasars”, ASP Vol 21, p. 191
Bushouse, H. A.: 1986, AJ 91, 255
Carico, D. P., Graham, J. R., Matthews, K. et al.:1990, ApJ 349, L39
Cavaliere A., Padovani P.: 1989, ApJ 340, L5
Cid Fernandes, R., Storchi-Bergmann, T., Schmitt, H.R.: 1998, MNRAS 297, 579
Colgate S.A.: 1967, ApJ 150, 163
Combes, F., Gerin, M.: 1985, A&A 150, 327
Combes, F. : 1988, in “Galactic and Extragalactic Star Formation”, ed. R. E. Pudritz and M. Fich, Kluwer, p. 475
Combes, F., Debbasch, F., Friedli, D., and Pfenniger, D.: 1990, A&A 233, 82
Combes, F., Elmegreen, B. G.: 1993, A&A, 271, 391
Combes, F. : 2000, in “Dynamics of Galaxies: From the Early Universe to the Present”, ed. F. Combes, G.A. Mamon, & V. Charmandaris, ASP Vol. 197, p. 15
Contopoulos, G. and Grosbol, P.: 1989 A&A Rev. 1, 261
Courvoisier, T. J.-L., Paltani, S., Walter, R.:1996, A&A 308, L17
Dahari, O.: 1984, AJ 89, 966
Dahari, O.: 1985, AJ 90, 1772
Dahari, O., DeRobertis M.: 1988, ApJ 331, 727
DeRobertis, M., Hayhoe, K., Yee, H. K. C.: 1996 AAS 189 109.04
Dultzin-Hacyan, D., Krongold, Y., Fuentes-Guridi, I., Marziani, P.: 1999, ApJ 513, L111
Duncan M.J., Shapiro S.L.: 1983, ApJ 268, 565
Ebisuzaki, T., Makino, J., Okumura, S. K.: 1991, Nature 354, 212

Eckart A., Genzel, R., Hofmann, R., Sams, B. J., Tacconi-Garman, L. E.:1993, ApJ 407, L77

Edwards A.C.: 1980, MNRAS 190, 757

Emsellem, E., Greusard, D., Combes, F. et al.: 2001, A&A 368, 52

Fabian A.C.: 1994, ARAA 32, 277

Fabian A.C., Sanders, J.S., Ettori, S. et al.: 2001, MNRAS 321, L33

Ferrarese, L., Merritt, D.: 2000, ApJ 539, L9

Frank J., Rees M.J.: 1976, MNRAS 176, 633

Fukushige, T., Ebisuzaki, T., Makino, J.: 1992, ApJ 396, L61

Gebhardt, K., Bender, R., Bower, G. et al.: 2000, ApJ 539, L13

Graham, J. R., Carico, D. P., Matthews, K., Neugebauer, G., Soifer, B. T., Wilson, T. D.: 1990, ApJ 354, L5

Haehnelt M.G., Rees M.J.: 1993, MNRAS 263, 168

Haehnelt M.G., Natarajan P., Rees M.J.: 1998, MNRAS 300, 817

Hasan, H., & Norman, C.A. 1990, ApJ, 361, 69

Hasan H., Pfenniger D., Norman C: 1993, ApJ 409, 91

Heckman T.M.: 1990, in “Paired and Interacting Galaxies” International Astronomical Union Colloquium No. 124 p 359

Hills J.G.: 1975, Nature 254, 295

Ho, L.C., Filippenko, A.V., Sargent, W.L.W.: 1997, ApJ 487, 568

Hunt L.K., Malkan M.A.: 1999 ApJ 516, 660

Hutchings, J. B., Neff S. G.: 1992 AJ 104, 1

Hutchings, J. B., Morris, S. C.: 1995, AJ 109, 928

Ishizuki S., Kawabe R., Ishiguro M. et al.: 1990 Nature, 344, 224

Jungwiert B., Combes, F., Axon, D. J., 1997, A&AS 125, 479

Kaastra J.S., Roos N.: 1992, A&A 254, 96

Kalnajs, A. J.: 1973, Proc. Astron. Soc. Australia 2, 174

Kauffmann, G., Haehnelt, M.: 2000, MNRAS 311, 576

Keel W.C., Kennicutt R.C., Hummel, E., van der Hulst J-M.: 1985, AJ 90, 708

Kim, D.-C., Veilleux, S., Sanders, D. B.: 1998 ApJ 508, 627

Knapen, J. H., Shlosman, I., Peletier R.F.: 2000, ApJ 529, 93

Laine S., Shlosman, I., Knapen, J.H., Peletier, R.F.: 2002, ApJ 567, 97

Laurikainen, E., Salo, H.: 1995, A&A 293, 683

Lawrence, A., Rowan-Robinson, M., Leech, K., Jones, D. H. P., Wall, J. V.: 1989, MNRAS 240, 329

Lehto H.J., Valtonen M.J.: 1996, ApJ 460, 207

Lynden-Bell, D., Kalnajs, A.J.:1972, MNRAS, 157, 1

Magorrian, J., Tremaine, S., Richstone, D., et al. 1998, AJ, 115, 2285

Martin P., Roy J-R.: 1994, ApJ 424, 599

Martini, P., Pogge, R.W.: 1999, AJ 118, 2646

McKenty J.: 1989, ApJ 343, 125

McLeod, K. K., Rieke, G. H.: 1995, ApJ 441, 96

Mihos J.C., Hernquist L.:1994 ApJ, 437, 611

Mihos, J.C., Hernquist, L.:1996, ApJ, 464, 641.

Mikkola, S.,Valtonen, M. J.: 1992, MNRAS 259, 115

Milosavljevic, M., Merritt, D.: 2001, ApJ 563, 34

Moles, M., Marquez, I., Perez, E.: 1995, ApJ 438, 604

Mulchaey J.S., Regan M.W.: 1997, ApJ 482, L135

Murphy, B. W., Cohn, H. N., Durisen, R. H.: 1991, ApJ 370, 60

Nakano T., Makino J.: 1999 ApJ 525, 77

Norman C., Silk J.: 1983, ApJ 266, 502

Norman C., Scoville N.Z.: 1988, ApJ 332, 124

Owen, F. N., Odea, C. P., Inoue, M., Eilek, J. A.:1985 ApJ 294, L85

Peletier, R. F., Knapen, J. H., Shlosman, I., et al.: 1999, ApJS 125, 363

Pietilä H.: 1998, ApJ 508, 669

Pfenniger, D., & Norman, C. 1990, ApJ, 363, 391

Phinney E.S.: 1994, in “Mass-transfer induced activity in galaxies” ed. I. Shlosman, Cambridge Univ. Press, p. 1

Pogge, R.W., Martini P.: 2002, ApJ 569, 624

Quinlan G.D.: 1996, New A. 1, 35

Quinlan G.D., Hernquist L.: 1997, New A. 2, 533

Raha, N., Sellwood, J. A., James, R. A., Kahn, F.: 1991, Nature 352, 411

Rauch K.P.: 1999, ApJ 514, 725

Regan, M. W., Mulchaey, J. S.: 1999 AJ 117, 2676

Roos N., Kaastra J.S., Hummel C.A.: 1993, ApJ 409, 130

Rubin V.C., Kenney J.D.P., Young J.S.:1997 AJ 113, 1250

Sakamoto, K., Okumura, S. K., Ishizuki, S., Scoville, N. Z.: 1999, ApJ 525, 691

Sanders D.B., Mirabel I.F.: 1996, ARAA 34, 749

Shaver, P. A., Wall, J. V., Kellermann, K. I., Jackson, C. A., Hawkins, M. R. S.: 1996, Nature 384, 439

Schmitt H.R.: 2001 AJ 122, 2243

Schmitt, H. R., Antonucci, R. R. J., Ulvestad, J. S. et al.: 2001, ApJ 555, 663

Schwarz, M. P.: 1981, ApJ 247, 77

Shlosman, I., Frank J., Begelman M.C.: 1989, Nature 338, 45

Shlosman, I., Peletier, R. F., Knapen, J. H. : 2000, ApJ 535, L83
Simkin S.M., Su H.J., Schwarz M.P.: 1980, ApJ, 237, 404
Spitzer L., Saslaw W.C.: 1966, ApJ 143, 400
Storrie-Lombardi L.J., Wolfe A.M.: 2000, ApJ 543, 552
Takalo L.O.: 1994, Vistas Astron. 38,77
Terlevich, R., Melnick, J., Moles, M.: 1987, in “Observational Evidence of Activity in Galaxies”, IAU 121, Kluwer Academic Publishers, Dordrecht, p.499
Toomre A.: 1977, ARAA 15, 437
van der Marel, R.P.: 1999 AJ 117, 744
Williams R. J. R., Baker, A. C., Perry, J.J.: 1999, MNRAS 310, 913
Wozniak H., Friedli, D., Martinet, L., Martin, P., Bratschi, P.: 1995, A&AS 111, 115
Young, P.: 1980 ApJ 242, 1232